The Klystron Engineering Model Development (KEMD) Task — A New Design for the Goldstone Solar System Radar (GSSR)

Lawrence Teitelbaum,* Roland Liou,† Yakov Vodonos,† Jose Velazco,† Kenneth Andrews,‡ and Dan Kelley▲

ABSTRACT. — The Goldstone Solar System Radar (GSSR) is one of the world's great planetary radar facilities. The heart of the GSSR is its high-power transmitter, which radiates ~450 kW from DSS-14, the Deep Space Network's 70-m antenna at Goldstone, by combining the output from two 250-kW klystrons. Klystrons are vacuum tube electron beam devices that are the key amplifying elements of most radio frequency telecommunications and radar transmitter systems. NASA's Science Mission Directorate sponsored the development of a new design for a 250-kW power, 50-MHz bandwidth, reliable klystron, intended to replace the aging operational devices that were developed in the mid-1990s. The design, developed in partnership with Communications & Power Industries, was verified by implementing and testing a first article prototype, the engineering model. Key elements of the design are new beam optics and focusing magnet, a seven-cavity RF body, and a modern collector able to reliably dissipate the full power of the electron beam. The first klystron based on the new VKX-7864C design was delivered to the DSN High-Power Transmitter Test Facility on November 1, 2016, the culmination of a six-year effort initiated to explore higher-resolution imaging of potentially hazardous near-Earth asteroids. The new design met or exceeded all requirements, including supporting advanced GSSR ranging modulations. The first article prototype was placed into operational service on July 26, 2017, after failure of one of the older klystrons, restoring the GSSR to full-power operations.

I. Introduction

The Goldstone Solar System Radar (GSSR), located at the Deep Space Network's (DSN's) Goldstone Deep Space Communications Complex (GDSCC), is one of the world's great planetary radar facilities. It takes advantage of the high gain and large collecting area of Deep Space Station–14 (DSS-14), the DSN's 70-m antenna at GDSCC, and utilizes extremely

* Tracking Systems and Applications Section.
† Communications Ground Systems Section.
‡ Communications Architectures and Research Section.
▲ Deep Space Network Project Office.

The research described in this publication was carried out by the Jet Propulsion Laboratory, California Institute of Technology, under a contract with the National Aeronautics and Space Administration.

low-noise receiving systems. Operating at X-band, at a center frequency of 8560 MHz, the GSSR is the most sensitive, fully steerable radar in the world, capable of observing complete target rise-to-set arcs over most of the sky. Recent GSSR observations include measurement of the spin state of Mercury [1,2], characterization and shape modeling of near-Earth asteroids (NEAs) [3], and determination of the trajectories of spacecraft orbiting the Moon [4].

The GSSR uses continuous-wave (CW) transmissions to measure the Doppler shift of reflected signals that results from the radial velocity and rotation of a target body. Ranging modulations are used to accurately measure the time delay of the reflected signals, from which distance can be inferred, and to produce high-resolution delay-Doppler images. Development of more advanced ranging modulations, in particular, wide-bandwidth chirp modulations over the full available transmitter bandwidth, have enabled 3.75-m-resolution delay-Doppler images of the lunar poles and NEAs and improved shape models, which are derived from sequences of delay-Doppler images. The GSSR can operate as a stand-alone monostatic radar system, with both transmission and reception at DSS-14, or in bistatic configurations, with echo reception at a second, independent antenna. Bistatic mode is used for close targets with short echo round-trip light times and to achieve higher sensitivity by pairing DSS-14 with larger collecting area radio telescopes like the 100-m Green Bank Telescope and the 305-m Arecibo Observatory. DSS-14 plays a unique role in the radar astronomy community as a steerable, nearly full-sky, high-gain, high-power illuminator capable of advanced ranging modulations.

The heart of the GSSR is its high-power transmitter, which is capable of radiating ~450 kW by low-loss power combining of the output from two 250-kW klystrons, vacuum tube electron beam devices that are the key amplifying elements of most radio frequency telecommunications and radar transmitter systems. Except for the advanced ranging modulations, the GSSR transmitter attained its present capability, configuration, and much of its underlying infrastructure by the early 1990s, shortly after DSS-14 was upgraded from 64 m to 70 m for the Voyager Neptune encounter [5]. In 1991, two new klystrons, designed specifically for the GSSR by Varian Associates to achieve higher power and better reliability [6], were installed, upgrading the GSSR to 450 kW. Unfortunately, the four klystrons delivered to the DSN based on this design, the model VKX-7864A, were not well-matched in group delay and were of insufficient bandwidth. Moreover, the reliability goals were not achieved: all four klystrons failed early in their intended lifetimes. A modified version of this design, the VKX-7864B [7], was developed by Varian's successor, Communications & Power Industries (CPI); key requirements were an output power of 250 kW, a bandwidth of 50 MHz, and a center frequency of 8560 MHz. Four new klystrons based on the B-series design were placed into service in the 1999–2000 timeframe. These klystrons have served the GSSR well, during a period when the number of radar observations per year has more than doubled. However, all have failed over the last ~10 years, requiring expensive and lengthy repairs and precipitating a number of "klystron sparing crises" that have reduced the availability of the DSN radar service or necessitated operation at less than full power. Clearly, a more reliable klystron was needed.

In 2010, the National Research Council issued its final *Defending Planet Earth* report [8], providing a strong rationale for a greater emphasis on detection, observation, precise orbit

determination, and characterization of NEAs. In 2011, Caltech's Keck Institute for Space Studies (KISS) initiated an in-depth study of the feasibility of retrieving and returning a NEA to the vicinity of Earth [9], leading to the formulation of the Asteroid Redirect Robotic Mission (ARRM) concept. JPL's Research and Technology Development (R&TD) program responded to these motivations in 2012–2013 by providing funding to explore the potential of a higher-resolution DSN radar capability and to develop a higher-bandwidth klystron design to enable the highest resolution compatible with the 200 MHz of frequency spectrum allocated for high-power radar transmission. Two studies were conducted by CPI. The first study simulated a number of designs in the trade space of (output power, bandwidth) with the goals of determining the maximum power that could be realized over the full 200-MHz bandwidth and the maximum bandwidth that could be achieved with a minimum output power of 250 kW across the full band. This study concluded that the best candidate for a new design that could achieve incremental, but significant, improvements in GSSR transmitter power and imaging resolution was a 250-kW, 120-MHz device. The Phase II study focused on a detailed preliminary design that could achieve this power and bandwidth, simulated the new design, and built and tested the critical wideband output circuit. CPI also provided a budgetary cost estimate for new klystrons based on this design that would serve as the basis of estimate for future advocacy with NASA. Figure 1 shows the major elements of a klystron: the electron gun, the multicavity RF body, the solenoid focusing magnet, the output circuit and vacuum window, and the collector, the beam dump for the spent electron beam.

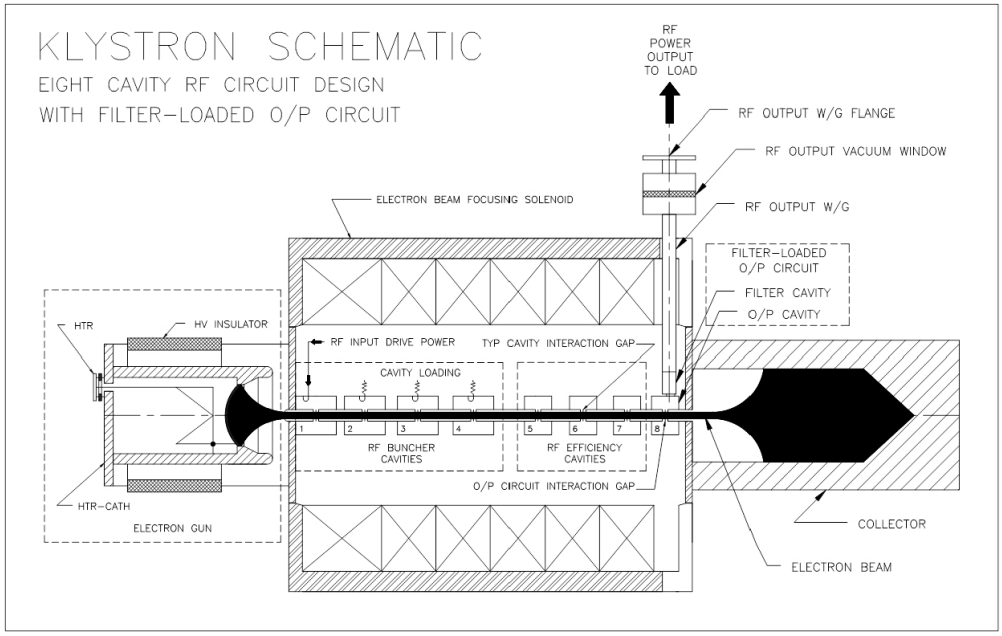

Figure 1. Klystron schematic. The major elements of a device are the electron gun, multicavity RF body, solenoid focusing magnet, output circuit and vacuum window, and collector. The electron beam (black) must be well confined in the RF body for high gain and reliability. The beam spreads after it exits the magnetic field; handling its power dissipation in the collector is crucial for a reliable device.

With confidence that a new klystron could be acquired with both better performance and higher reliability, a conceptual design was developed for a comprehensive GSSR uplink modernization on DSS-14. The guidelines for the effort were:

(1) Implement an entirely new end-to-end radar transmitter system, including modern high-voltage power supplies and monitor and control equipment.

(2) Achieve a factor-of-three improvement in radar imaging to ~1 m, human-scale and relevant for the characterization of the ~10-m NEA targets of interest to the ARRM mission, by using chirp modulation over a 120-MHz bandwidth, three times wider than the current GSSR highest-resolution mode.

(3) Create a pathway to a factor-of-two improvement in transmitter power, to ~1 MW, by power combining the output of four klystrons.

(4) Conform to accommodation constraints of the upper structure of the 70-m antennas and infrastructure constraints of the DSN complexes, ensuring that a Southern Hemisphere radar could be implemented at DSS-43, the DSN 70-m antenna at the Canberra Deep Space Communications Complex (CDSCC), as well as at Goldstone.

After preliminary presentations at JPL and a baseline commitments and cost review led by the Communications, Tracking, and Radar Division (33), in 2014 JPL was invited to brief NASA on the concept for a NASA solar system radar. NASA asked JPL to address:

(1) DSN radar service reliability and availability.

(2) Expansion to the Southern Hemisphere for complete sky coverage.

(3) Higher-resolution imaging.

The briefing did not convince NASA to invest in a comprehensive GSSR uplink modernization, a duplicate capability in the Southern Hemisphere on DSS-43, or a higher-resolution capability for the GSSR. However, NASA's Science Mission Directorate (SMD), the NASA program office that sponsors use of the GSSR for scientific observations, believed "something has to be done about the klystrons" and provided funding to develop a new 250-kW, 50-MHz design and verify it by implementing a first article prototype. The three-year Klystron Engineering Model Development (KEMD) task resulted from this SMD investment.

II. NASA Task Plan, Requirements and Statement of Work, CPI Subcontract

Three key documents were developed in parallel because of their interdependence and the need for consistency in their schedules and deliverables:

(1) The NASA Task Plan, which spelled out JPL's obligations to the SMD sponsor and defined the KEMD task as the

(i) design and nonrecurring engineering required to produce a modern, high-reliability, 250-kW, 50-MHz bandwidth, X-band, fixed-tuned klystron, followed by

(ii) implementation of a first article prototype to verify the design, the engineering model.

(2) The detailed technical specifications document that established requirements for the new klystron, quality assurance provisions, and test methods.

(3) The subcontract with CPI, which was again selected as the sole-source provider capable of developing a new device.

The subcontract was entered into and work commenced at the end of April 2015.

As an evolution from the earlier design, with identical key requirements for center frequency, output power, and bandwidth, CPI assigned the model number VKX-7864C to the new klystron. CPI had recently collaborated with JPL [10] on the successful design of a new 100-kW klystron (VKX-7976A) to power an 80-kW transmitter system for DSN 34-m beam-waveguide (BWG) antennas, providing a telecommunications X-band uplink capability equivalent to the 20-kW X-band capability on the DSN 70-m antennas. Because of this experience, the technical specifications document for the GSSR VKX-7864C klystron amplifier was influenced by lessons learned during the 100-kW klystron development as well as the earlier B-series design and the field history from more than a decade of GSSR operations.

A detailed statement of work (SOW) was incorporated into the CPI subcontract, guiding the new klystron development, defining its objectives and schedule, and establishing partial payment milestones. At a high level, the SOW consisted of:

(1) Reviewing the technical specifications document.

(2) Performing nonrecurring engineering (NRE), including reviewing the performance, field history, and build methodology of the VKX-7864B devices.

(3) Fabricating and testing the prototype.

(4) Meeting JPL quality assurance standards and providing for witnessed acceptance testing prior to delivering the device to the DSN High-Power Transmitter Test Facility (HPTTF) at the Venus site at GDSCC.

The NRE was based on new simulation codes and techniques not available at the time of the B-series design, nearly 20 years ago. To validate the VKX-7864C design, CPI focused on a number of key elements:

- **Electron beam optics**. A well-focused electron beam and better beam confinement as electrons traverse multiple RF cavities to achieve high gain would be required to improve performance and reliability. One of the failure modes of the GSSR klystrons has been singed cavity drift tube tips, indicating loss of control and confinement of the electron beam.
- **RF body multicavity design.** Employ progressively higher-fidelity large signal codes to establish the electrical design parameters and the number of cavities, and validate performance of a wideband output circuit to achieve 250-kW output power over a 50-MHz bandwidth centered at 8560 MHz with less than 1 dB variation across the band. Synthesize the geometry of the cavities and output circuit and fabricate and cold-test the cavities to verify the design.

- **Solenoid magnet.** Use high-fidelity signal codes to determine the magnetic field required to optimize beam focusing at full RF performance.
- **Output waveguide.** Review the electrical and mechanical design to ensure a low-voltage standing-wave ratio (VSWR) between the output circuit and output window and sufficient cooling to maintain RF stability.
- **Isolated collector.** Review the existing collector electrical, thermal, and mechanical design and propose changes to improve reliability, thermal performance, and mechanical stability, and eliminate shorting to ground. The collector was the least reliable component of the VKX-7864B design, resulting in multiple tube failures.
- **Electron gun.** Review the existing VKX-7864B electron gun assembly, which was also used in the VKX-7976A 100-kW klystron, to validate the electron beam diameter used in all large-signal simulations. The electron gun was a reliable element in the GSSR klystrons and planned to be used in the new device.
- **Output window.** Review the existing design to ensure it can support the 250-kW output power and 50-MHz bandwidth requirements, and modify if necessary.
- **GSSR operational modes.** Review current GSSR operational modes and new ranging modulations to ensure design revisions introduced in the VKX-7864C will support them with improved lifetime and reliability.

The NRE phase would conclude with a final review at the CPI facility in Palo Alto, California, establishing the VKX-7864C design and preparing for implementation of the first article prototype.

III. Preliminary and Critical Design

The nine-month design phase of the KEMD task, which started as soon as the CPI subcontract was in place, consisted of preliminary design, critical design, and then final resolution of outstanding action items that marked the transition to implementation of the engineering model. Two preliminary design reviews were held at CPI in July and September 2015, respectively; the critical design review (CDR) took place at CPI in October 2015. The core JPL KEMD technical team and the Goldstone lead GSSR high-power transmitter engineer attended the reviews at CPI. Closeout of CDR action items, including finalizing all elements of the new design, transpired in November and December 2015, and January 2016. This section will highlight the key features that distinguish the VKX-7864C klystron from the earlier design.

Whereas the existing VKX-7864B electron gun, its electron beam, beam propagation through the RF cavities, and beam confinement by the solenoid magnet were developed in the late 1980s using Varian's beam analyzer, today CPI uses sophisticated computer codes to design and analyze new beam optics systems [11,12]. Software simulation enables rapid parameter variation and optimization and reduces sensor measurement errors that affected the beam analyzer approach. The only disadvantage of the simulation technique is that additional computer codes, such as ANSYS, are required for thermal analysis of mechanical electron gun structures to ensure dimensional consistency between "cold" mechanical

design and the “hot” dimensions used during beam optics simulation. CPI validated this method on the existing gun design by comparison with older results achieved with the Varian beam analyzer.

Key gun design parameters were varied to optimize the electron beam. A minor modification to the electron gun, a small increase in the inside diameter of the input pole piece aperture, increased the beam fill factor and significantly reduced the beam scallop. Figure 2 compares the optimized beam in the new klystron to the simulated beam from the existing design.

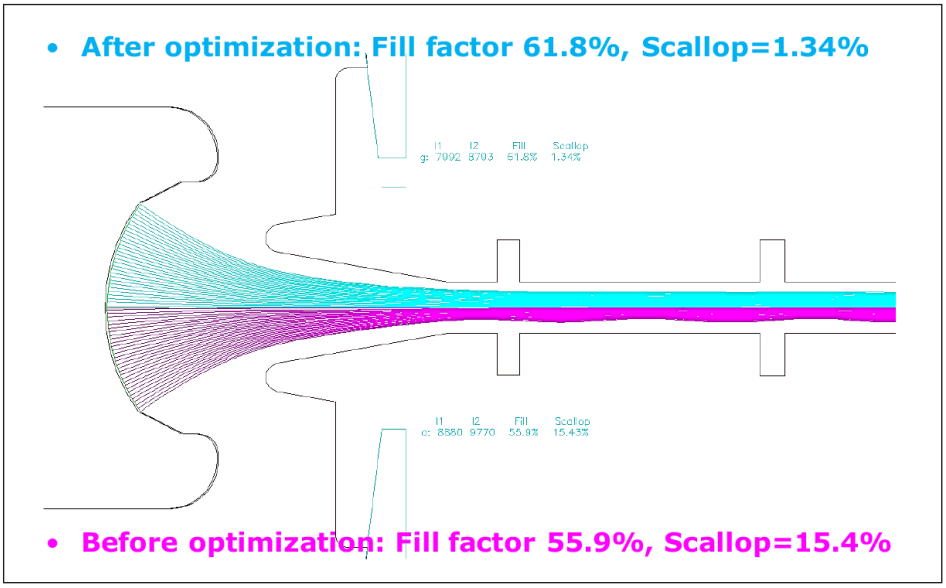

Figure 2. VKX-7864C optimized electron beam with increased fill factor and dramatically reduced beam scallop. The beam enters the RF body and focusing magnet from the left. The first two accelerating RF cavities are shown. Beam size is larger on average, improving efficiency and gain, but the maximum diameter is reduced, improving beam confinement and reliability.

The modified gun and optimized electron beam, combined with the new RF circuit and magnet, will provide better beam confinement and improve performance and reliability by

(1) Increasing gain and efficiency.

(2) Minimizing potentially damaging body current during ranging modulations such as binary phase code (BPC) and chirp.

(3) Minimizing potential thermal damage from beam interception by RF cavity drift tips.

Improved mechanical stability between the magnet and klystron will maintain electron beam/magnet alignment when the antenna tips in elevation away from zenith pointing and the device is subjected to mechanical stress from gravitational loading.

Extensive simulations using the optimized beam were employed to design a new, seven-cavity RF body. Compared to the VKX-7864B design, an additional cavity was added to increase

klystron gain and efficiency. A new single-gap output circuit was designed to ensure the klystron would meet its power requirements across the full band. A filter-loaded output circuit that had been designed in the initial trade study to achieve 120-MHz bandwidth was not needed to meet the 50-MHz requirement. The HFSS High-Frequency Structural Simulator code, the ANSYS thermal and mechanical tools, and the CFX computational fluid dynamics program were incorporated into a software tool flow to analyze electromagnetic, mechanical, cooling circuit, and thermal effects in an integrated, iterative, self-consistent manner. A cut-away view of the three-dimensional SolidWorks model of the final design is shown in Figure 3.

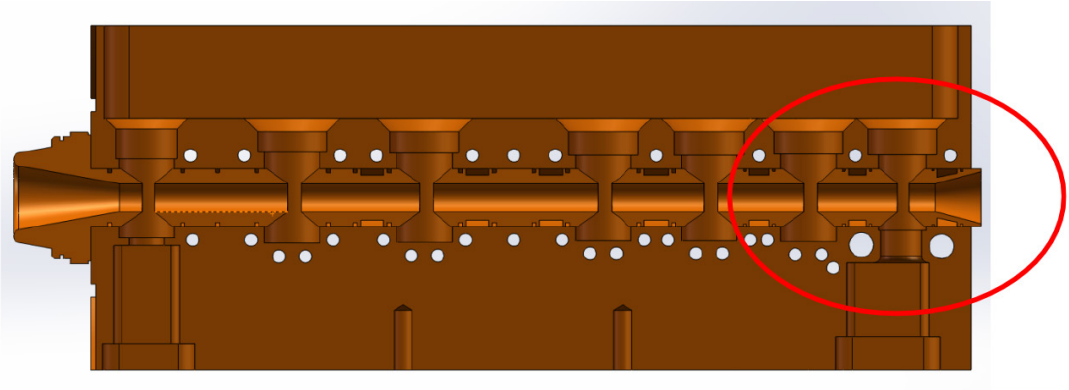

Figure 3. VKX-7864C seven-cavity RF body. The electron beam enters from the left. Cooling channels are shown. The red oval encloses the penultimate cavity, which uses a copper/molybdenum composite for better thermal stability, and the new output cavity; grooves were added to high-flow cooling channels to reduce pressure gradients and susceptibility to cavitation.

Another innovation was the use of a copper/molybdenum composite approach for the drift tube tips. The use of composite material in construction of the drift tubes improves thermal stability by reducing structural dimensional changes caused by changes in temperature, which reduces thermal detuning that compromises RF performance.

Detailed mechanical and thermal modeling was used for all major elements of the new design. A new RF body water channel circuit was developed to provide conservative heat dissipation margins and reduce the risk of cavitation. Figure 4, which shows streamlines for the fluid flow in the water circuit at a relative pressure drop of 50 psi across the circuit at a water flow of 18 gallons per minute, is an example of the sophistication and comprehensiveness of the integrated software tool flow used for the simulations.

In order to accommodate the increased length of the new seven-cavity RF body, a magnet was designed with an axial magnetic field "stretched" along the *z*-dimension. Figure 5 compares the magnetic field for the new design to an analytic representation of the field in the VKX-7864B model; the simulated field was also compared to test data provided by the manufacturer for the existing magnet. Access and coil taps were added to the magnet coils to allow field adjustment in order to control the beam diameter in the penultimate cavity and output circuit region of the klystron body.

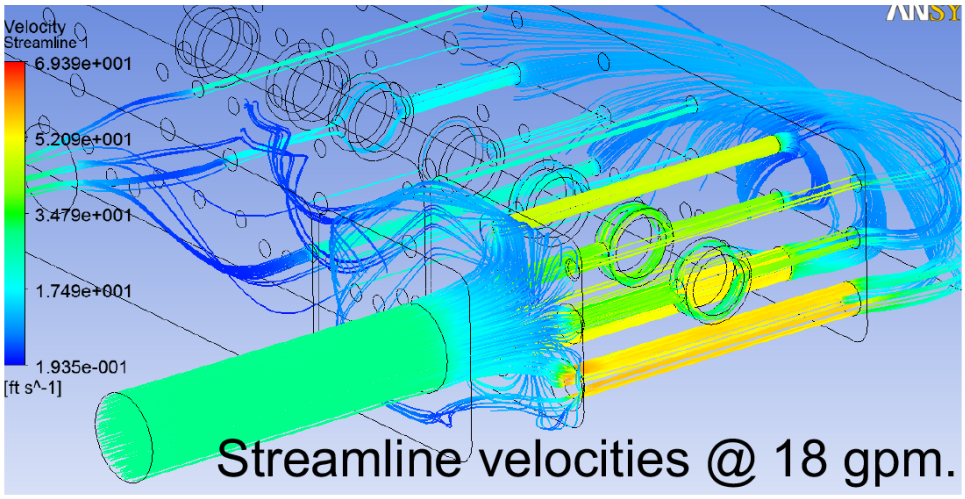

Figure 4. Computational fluid dynamics were used to simulate and analyze water flow, thermal effects, and mechanical response to stresses. Water circuit streamlines are shown at a flow rate of 18 gpm with an improved pressure drop of 50 psi.

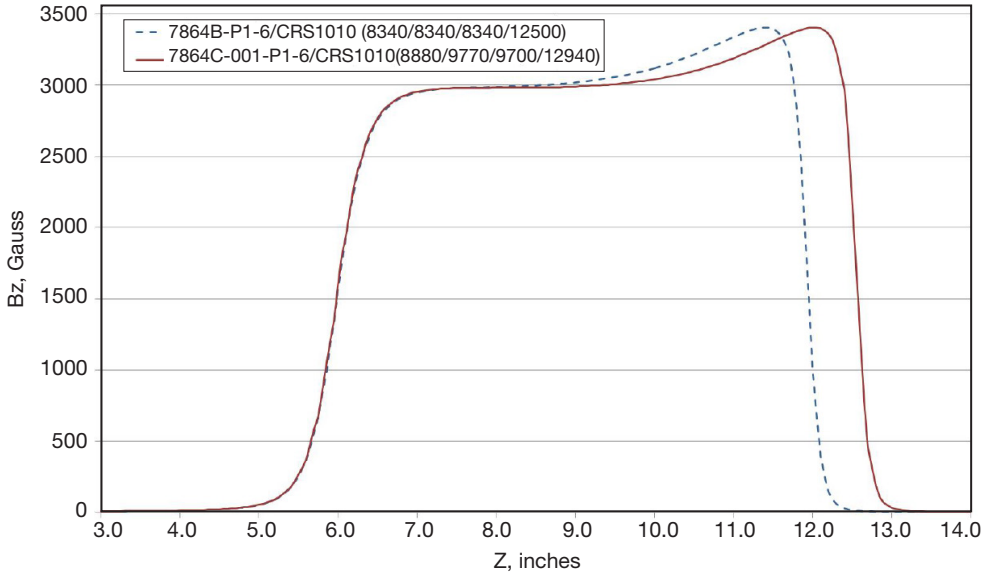

Figure 5. VKX-7864C stretched magnetic field compared to earlier design. Coil taps to the multiple coils in the solenoid enable field adjustment for better beam confinement.

Because of the multiple collector failures that had occurred for the operational fleet of GSSR klystrons, CPI expended a major effort designing a more reliable collector. The geometry, including a cone-shaped final section, is shown in Figure 6.

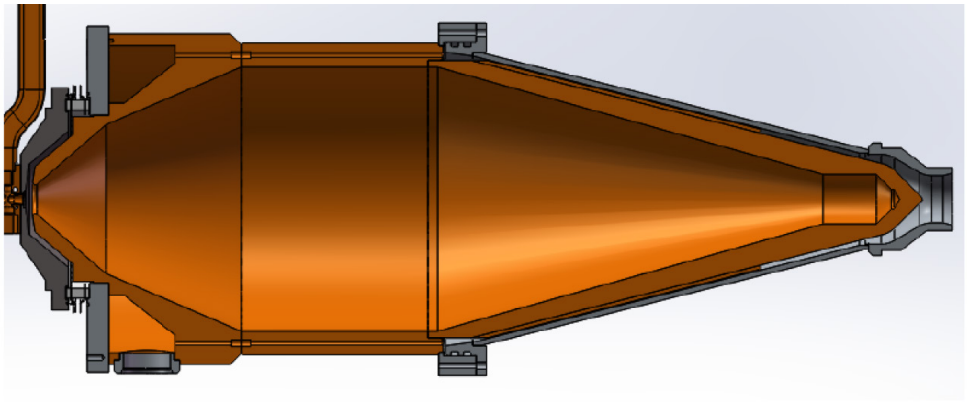

Figure 6. VKX-7864C collector internal structure, featuring fewer braze joints (vertical lines) and a cone-shaped final section for more evenly distributed energy dissipation from the spent electron beam which, combined with an improved cooling circuit, will increase reliability.

Based on recent CPI collector designs for high-power, CW devices, the design features longer, thus fewer, sections to reduce the number of braze joints and optimize their locations. In particular, the initial strike of the diverging electron beam as it exits the focusing magnetic field occurs in the large cylindrical section away from the braze joints. The cone-shaped collector distributes energy dissipation from secondary electron scattering across a larger surface area, reducing energy density and ameliorating the thermal management problem. The standard cone-shaped end section is covered with a dense circuit of cooling channels over its entire exterior surface, a major modification to the cooling circuit in the VKX-7864B klystron, which terminated in an Archimedes spiral at the flat end of that device [6]. The collector was designed to dissipate the full electron beam power in the absence of RF drive, the so-called direct current (DC) beam. This is the most thermally stressful condition: without application of RF drive, no power is transferred from the electron beam to the amplified klystron output signal. The development also benefited from an opportunity to inspect a damaged collector from one of two GSSR operational units that had failed and been returned to CPI for a major repair.

The same set of electromagnetic, mechanical, and thermal modeling tools was used to simulate and verify the VKX-7864B beryllium oxide (BeO) output window with the revised beam optics and RF circuit, and to optimize it for use in the new design. BeO is a good structural ceramic for microwave applications because it is an excellent insulator with very high thermal conductivity. Minor changes to the window geometry resulted in a reduced VSWR, ensuring good power transfer across the output window, with low sensitivity to potential variation in BeO dielectric constant or dimensional tolerances. Peak voltage gradients can be handled without inducing dielectric breakdown that might result in failure due to arcing. An electromagnetic mode search found no potentially harmful ghost or trapped waveguide modes that could cause excessive power dissipation. Thermal analysis showed the window will effectively dissipate heat from peak electric fields and maintain a thermally stable, steady-state temperature profile. The width of the copper sleeve that encloses the BeO win-

dow ceramic was selected to limit mechanical stress in response to cooling water pressure, which could otherwise affect performance and reliability. The braze process and fixture method for fabricating the window were updated to current best practice to improve braze joint quality and further reduce vulnerability to arcing in the high-field gradient region.

The output waveguide is an important interface between the final RF output cavity and the output vacuum window. The output waveguide for the VKX-7864B design featured an S-shaped section that was bent from custom WR-125 waveguide made from oxygen-free electronic (OFE) copper supplied by JPL. A black burn mark had been found in the bend region of the waveguide of one of the failed klystrons returned to CPI for repair. Simulations similar to those performed for the output window showed a low VSWR, indicating a good match, and ruled out trapped waveguide modes, verifying the electromagnetic design. Inadequate cooling or susceptibility to mechanical stress from poorly understood environmental conditions in the antenna were hypothesized as vulnerabilities in the existing devices. The mechanical design was revised to use a machined clamshell assembly method to improve the internal geometry and increase the cooling capacity, which will result in lower VSWR, better RF performance repeatability between klystrons based on the same design, and higher reliability. The SolidWorks model of the output waveguide is shown in Figure 7.

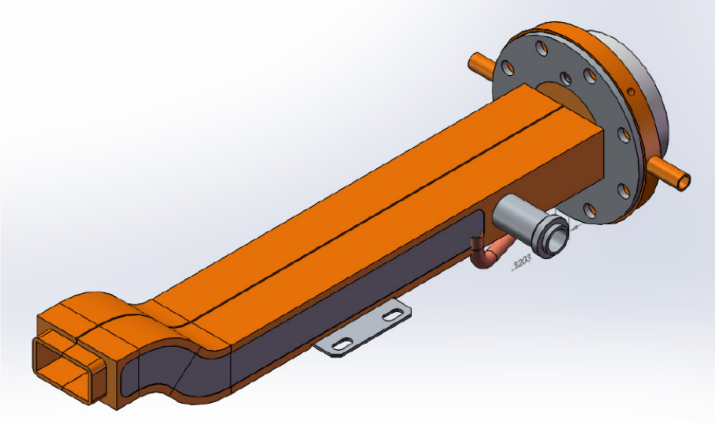

Figure 7. Machined clamshell output waveguide assembly.

Figure 8 shows the complete SolidWorks model of the seal-in assembly for the final design. Except for the solenoid magnet and the structural support enclosure for the device, the seal-in assembly includes all the key elements of the VKX-7864C klystron: the electron gun, the seven-cavity RF body, the clamshell output waveguide, the output vacuum window, and the radically redesigned collector. The dense collector cooling channel circuit on the cone section exterior surface can be seen in the figure. Fabrication, subassembly test and integration, and exhaust of the final seal-in assembly is a major milestone in the implementation phase of the klystron. A SolidWorks model of the complete klystron/magnet was used for final validation of form and fit, including modeling of the final hardware layout, support enclosure, and lifting fixtures. With design complete, detailed drawings and the bill of materials (BOM) listing were developed, marking the transition from design to implementation.

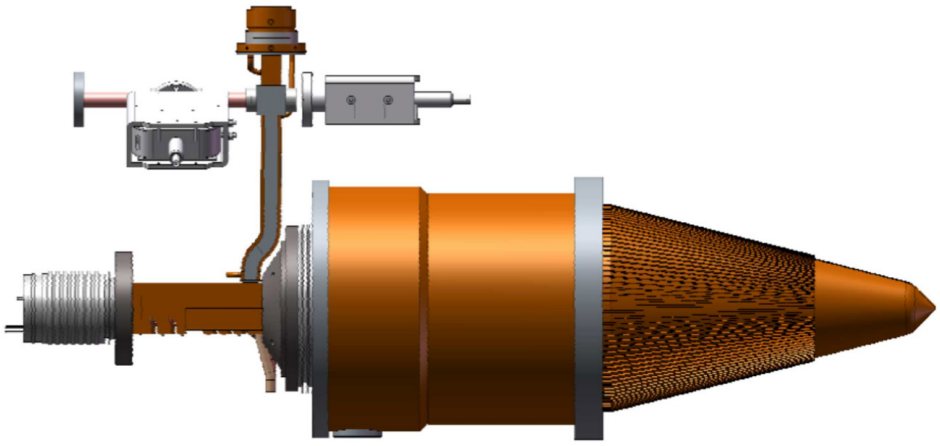

Figure 8. VKX-7864C seal-in assembly for the final design.

IV. Implementation

After closing remaining open action items from the CDR, the implementation phase of the first article prototype formally commenced near the end of January 2016 with the initiation of long-lead procurements. Implementation consists of

(1) Fabrication and cold-testing of subassemblies.

(2) Fabrication, integration and final brazing, and cold-testing of the RF body.

(3) Integration of the electron gun, the RF body, the output waveguide and window, and the collector to produce the seal-in assembly.

(4) Processing the seal-in assembly through the exhaust cycle.

(5) Integration of the magnet and dress hardware with the seal-in assembly.

(6) High-power DC, RF, and final testing of the complete device.

Due to a drawing revision control issue, a key supplier initially provided CPI incorrect collector copper forgings. Although this caused a schedule delay, the supplier made good, with no cost impact to the subcontract. The implementation phase, including testing, witnessed acceptance testing during the customer source inspection (CSI), preparation for shipment, and final inspection, took approximately 10 months, concluding with delivery to the Goldstone HPTTF on November 1, 2016. CPI assigned serial number (SN) 110 to the first VKX-7864C model klystron.

Prior to assembly and final brazing of the RF body, a microcomputed tomography (CT) scan of the composite drift tube tips was performed to assess the quality of the braze joints at the interfaces between the copper and molybdenum materials. A number of minor defects, braze voids, were revealed by the CT scan. CPI's analysis of the braze voids indicated that they would not introduce stress in the composite assemblies, affect the quality of the vacuum, or significantly alter the thermal transfer of heat away from the drift tips. Based on

CPI's assessment of low risk and a simple mitigation, longer exhaust processing to bake out gas trapped in a braze void, JPL decided to use the composite drift tube tips in the penultimate cavity of the prototype.

The as-built seal-in assembly is shown in Figure 9, both before and after processing through the exhaust cycle. It can be compared to the final design SolidWorks model in Figure 8.

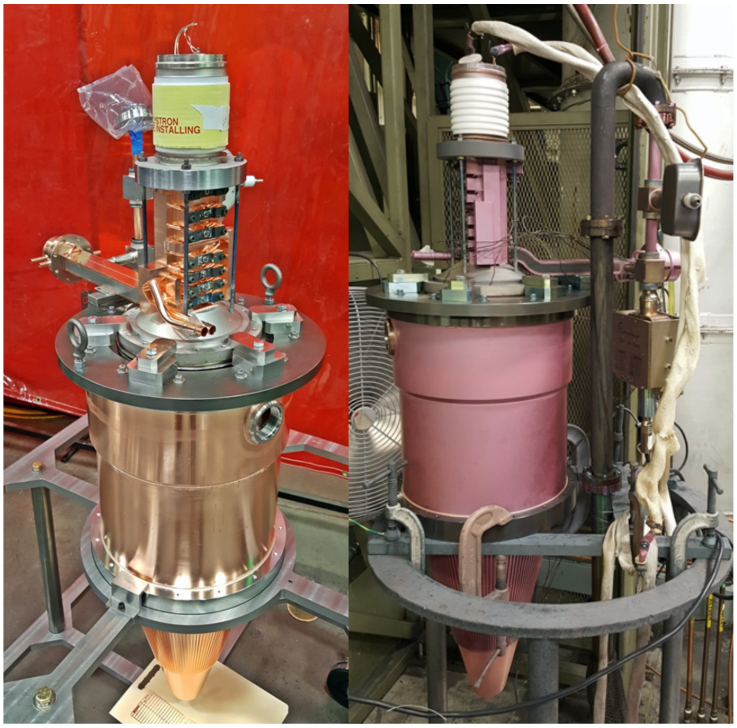

Figure 9. As-built seal-in assembly before (left) and after completion (right) of the exhaust cycle. Color change is normal during exhaust and does not affect klystron performance.

Exhaust processing started on August 27, 2016, proceeding through a series of preliminary leak checks, activation of the electron gun cathode, measurement of residual trace gases remaining throughout bakeout, and final verification of the quality of the device vacuum. The tube color turned from pristine copper to lavender early in the exhaust cycle, due to a poor external guard vacuum in the bakeout oven, which was recovered shortly afterward. Color change is normal during exhaust and does not affect klystron performance. Figure 10 shows the low residual trace gas partial pressures and the vacuum at the conclusion of the exhaust cycle on September 8, 2016. A modern vacuum-ion pump and pump controller, manufactured by Gamma Vacuum, is used in the VKX-7864C klystron to monitor and maintain vacuum. The pressure measured by the vacuum-ion pump was 8.6×10^{-11} torr with the cathode heater filament powered off and 1.7×10^{-9} torr with filament power on and the cathode activated. This is an excellent vacuum and evidence of a healthy klystron..

The seal-in assembly is integrated with the magnet and partially dressed for installation in the test stand for DC processing, RF processing, and final testing. Figure 11 shows the new

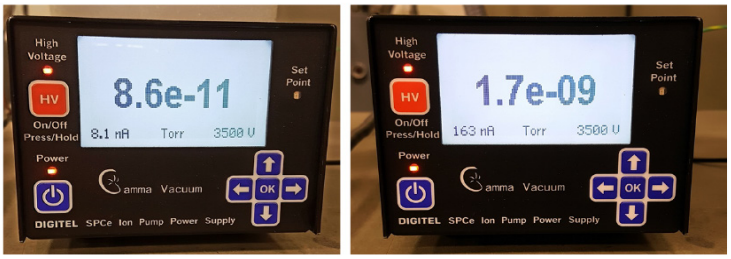

(a) (b)

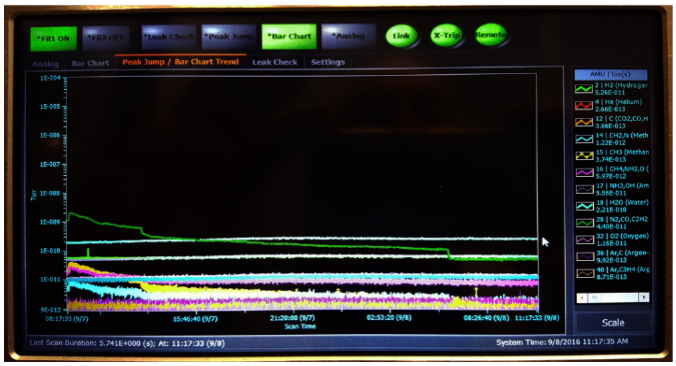

(c)

Figure 10. Excellent vacuum (a) and (b) and low residual trace gas partial pressures (c) were measured during exhaust (bakeout). The top green trace, moving downward, is carbon monoxide out-gassing from the cathode with its heater filament power on, indicating very low partial pressure. The vacuum is excellent with filament power off (a) and when the cathode is activated (b).

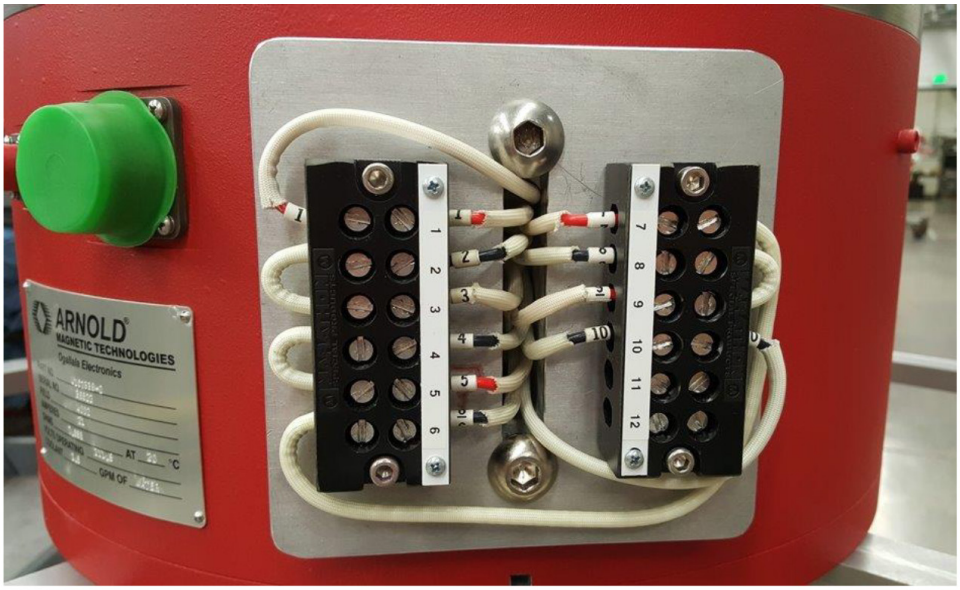

Figure 11. Terminal block of the new magnet, providing independent current adjustment of the five magnet coils to explore tailoring the magnetic field to improve electron beam confinement.

magnet, in particular, the terminal block that allows adjustment of the currents in the five magnet coils, a feature added to the first article prototype to explore fine-tuning of the magnetic field for better control of the beam diameter as electrons traverse the vacuum beam tunnel. This feature will be removed in future production units.

DC processing followed completion of the exhaust cycle and hardware installation and consists of methodically bringing the device up to full electron beam voltage while monitoring beam current, body current, potentially harmful X-ray production, and vacuum. The klystron is designed to produce at least 250 kW of output power at a beam voltage not to exceed 53 kV. Operating at 48 kV beam voltage, a set of infrared thermal images was taken to measure the collector temperature distribution, verifying the heat dissipation and thermal performance of the new design. An example is shown in Figure 12(a). These images indicated a minor tilt of the initial beam impact position. However, there was only a ~2.5 deg C variation of the maximum collector temperature across the entire assembly. During early RF processing at a beam voltage of 49.3 kV producing an output power of ~180 kW, as seen in Figure 12(b), the initial beam impact moves closer to the RF body, away from the braze joints as designed, the heat dissipation is more uniform across the collector, and the maximum temperature is ~10 deg C lower. No anomalous hot spots were discernible at any stage of the processing.

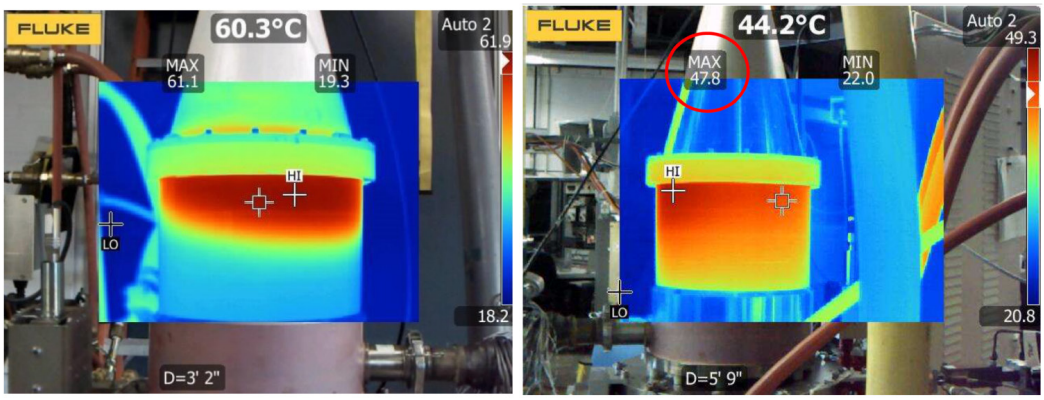

(a) (b)

Figure 12. Infrared thermal images of the VKX-7864C collector during (a) DC and (b) RF processing, at an output power of ~180 kW. The temperature distribution is much more uniform with drive power on. The collector is designed to thermally dissipate the full DC beam power.

RF processing continued, gradually increasing beam voltage and increasing RF input drive power to saturation, progressing slowly while maintaining excellent vacuum and low body current, tuning the klystron cavities to achieve the desired bandpass. Early output power measurements showed a flat bandpass and excellent gain, >49 dB, already surpassing the requirement. RF processing was completed on October 3, 2016. Initial data at full beam voltage and drive power showed the new klystron met all basic performance requirements, achieving full RF output power across the band. There were no detectable X-rays, even without the klystron lead shielding jacket, which would be added during final dress assembly when the klystron was prepared for final inspection and shipment.

V. CPI Final Testing and JPL Acceptance Testing at the HPTTF

Another CPI obligation under the subcontract was preparation, and submission for JPL concurrence, of a test procedure to verify that the first article prototype of the VKX-7864C klystron met all performance requirements in the technical specifications document. CPI final testing consisted of:

(1) Electrical performance testing to establish the name plate values (NPVs) for operating voltages and currents, to determine cooling flow rates for the RF body, output window, and collector, and to demonstrate leakage-free operation at hydrostatic pressure.

(2) RF performance testing to measure gain, efficiency, body current, output power as a function of frequency, RF input drive power for saturation, and output power variation over the central 18 MHz of the bandpass.

(3) A number of first-article tests to establish the phase sensitivity to deviations in operating voltages and currents from their NPV values or temperature excursions from typical environmental conditions.

The core JPL KEMD technical team travelled to CPI for witnessed acceptance testing during the CSI on October 19–20, 2016, marking completion of CPI testing. The final test results for SN 110 were certified by CPI on October 26 and distributed to JPL on October 28, 2016.

Figure 13 shows a key result, the VKX-7864C measured output power P_o as a function of frequency over the required 50-MHz band centered at 8560 MHz. The NPV operating voltages and currents established during testing are listed in the upper left corner of the figure, in particular, electron beam voltage E_b = 52.5 kV, RF input drive power P_d = 1.82 W, cathode heater filament voltage E_F = 10.0 V, and solenoid magnet current I_M = 22.0 A. The peak output power at NPV values is 285 kW. P_o exceeds 250 kW across the full 50-MHz band centered at 8560 MHz, meeting requirements, and is symmetric about the center frequency. The spectrum is nearly flat across the central 18 MHz, with a P_o variation of less than 0.1 dB. This performance significantly surpasses that of the earlier design. Although P_o starts to roll off sharply past the design-bandwidth edges at 8535 and 8585 MHz, the VKX-7864C design produces greater than 200 kW over nearly 80 MHz centered at 8560 MHz, perhaps enabling a factor-of-two improvement in range resolution for high-SNR targets. A modification to the output circuit might extend the bandwidth to a full 80 MHz.

Figure 14 shows the VKX-7864C output power P_o as a function of frequency for different RF input drive power levels, up to the NPV value P_d = 1.82 W. The electron beam voltage E_b and beam current I_b were set to their NPV values for all measurements — see Figure 13. Also shown are the peak output power and the body current I_{by} for each value of P_d. The body current with RF input drive at the center frequency F_o = 8560 MHz meets the not-to-exceed 50 mA requirement with margin. I_{by} without drive was 5.5 mA. Low body current is a strong indication of good beam confinement, an important design goal, and is critical for a reliable klystron and for long operational lifetime in the field. The VKX-7864C klystron achieves its peak output power, its full bandwidth, and its flattest and most symmetrical spectrum at NPV RF input drive power.

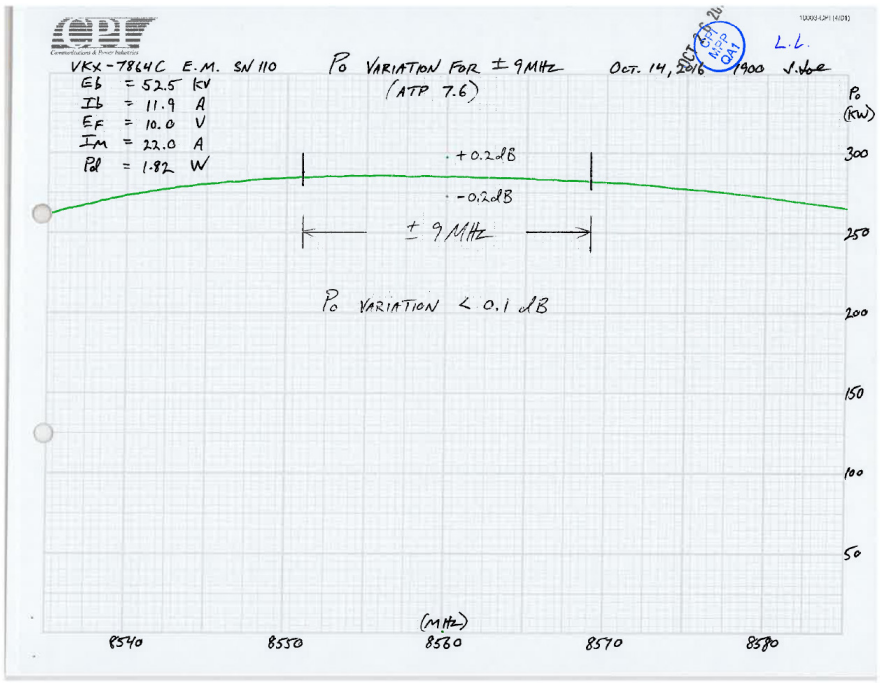

Figure 13. Output power P_o as a function of frequency over the 50-MHz band centered at 8560 MHz. NPV values are shown in the upper left of the figure. The spectrum is nearly flat across the central 18 MHz and exceeds the 250 kW requirement across the full band. The peak output power is 285 kW.

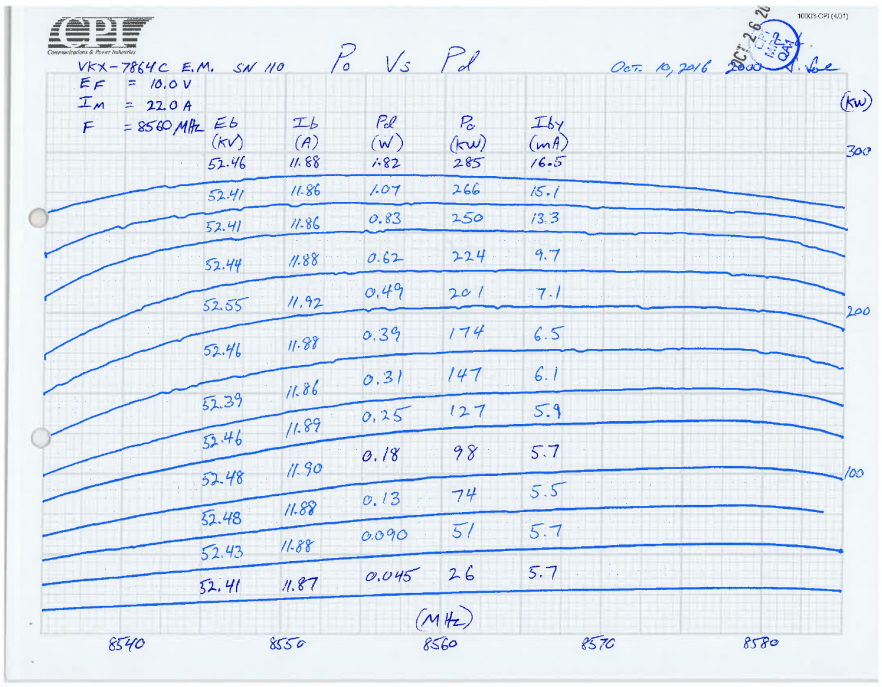

Figure 14. P_o as a function of frequency for different values of RF drive power P_d and NPV values for beam voltage E_b and solenoid magnet current I_M. The VKX-7864C klystron achieves its peak output power, full bandwidth, and flattest spectrum at NPV P_d = 1.82 W.

After final testing and the CSI, during final dress assembly the klystron was outfitted with its lead shielding jacket, equipped with CPI's characteristic red "strongback" structural support, and integrated with its solenoid magnet to produce a deliverable product. Figure 15 shows VKX-7864C SN 110, including lifting fixtures, being packed and prepared for shipment, with three of the key CPI design engineers who contributed to the project.

Figure 15. VKX-7864C SN 110 ready for shipment, with three of the key CPI engineers who contributed to the project: Brad Stockwell; Edward Eisen, who led the development; and Rasheda Begum.

JPL acceptance testing consists of repeating a subset of the CPI test measurements at the Goldstone HPTTF. JPL acceptance testing verifies that the device survived transport, confirms that the new klystron can be operated as an element of the GSSR transmitter system on DSS-14, and is an important milestone for JPL transmitter engineering and GDSCC high-power transmitter operations taking ownership of the device, able to operate it safely independent of CPI engineering support.

JPL acceptance testing was slated to begin shortly after delivery of the klystron to the Goldstone HPTTF on November 1, 2016. However, the testbed can only be configured for testing one tube type at a time and was committed to higher-priority testing of S-band klystrons needed for Voyager uplink from DSS-43. S-band testing was completed on April 22, 2017, the testbed was converted to the 8560-MHz high-power configuration, SN 110 was installed in the test socket, and testing commenced on May 11, 2017. The lead KEMD design engineer from CPI participated remotely during early testing. Safety interlocks were verified and the klystron DC beam was systematically brought up to NPV value while monitoring body and vacuum current. A number of testbed problems needed to be resolved to operate at the high beam voltage required for a 250-kW tube. Approaching DC beam NPV, at E_b = 43 kV, the klystron performed nominally with low body current, I_{by} =

4.6 mA, and a low vacuum current of 0.02 µA. On May 17, 2017, the first article prototype achieved full 250-kW output power with RF drive. The CPI lead development engineer traveled to GDSCC and participated with the core JPL KEMD technical team in acceptance testing and initial performance testing on May 22–23, 2017. The first full-power tests in CW mode at 8560 MHz achieved output power P_o = 276 kW with a body current I_{by} = 18.7 mA and a measured thermal power dissipation of 7.61 kW. The final DC beam test measurements recorded a body current I_{by} = 5.9 mA and a temperature increase of 0.02 deg C at the body cooling circuit inlet and outlet ports, corresponding to a thermal power dissipation of 0.01 kW. A modest experimental test setup was developed to measure these small temperature changes and the associated power dissipation, motivated by the interest in verifying the new cooling circuit and overall thermal design.

Figure 16 shows P_o as a function of time, implicitly as a function of frequency, during a linear frequency sweep over the design bandwidth from 8535 to 8585 MHz. The purple trace shows frequency as a function of time; the blue upper trace shows the output power. The frequency sweep was conducted after a peak output power of 285 kW was measured at 8560 MHz, band center frequency. Compare to Figure 13, measured at CPI prior to delivery. The measurement at the HPTTF shows the symmetry of the output power about the center frequency that was exhibited in the CPI final test data.

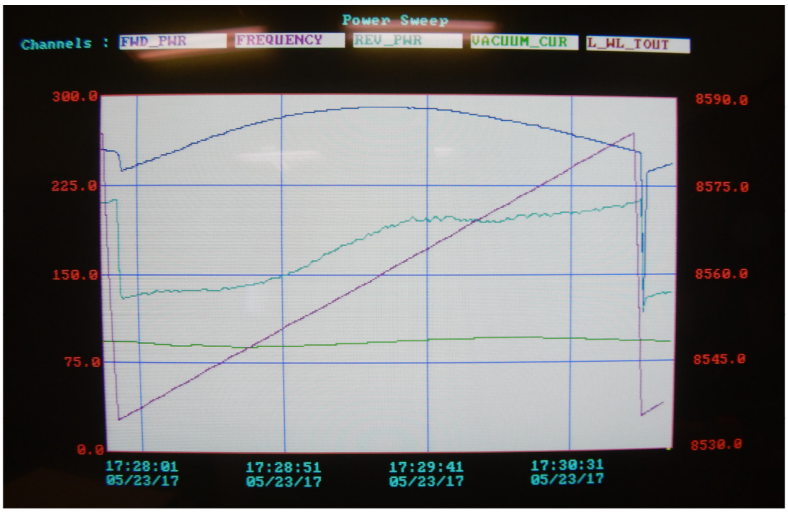

Figure 16. Output power frequency sweep measured at the High-Power Transmitter Test Facility (HPTTF).

A solenoid current experiment to run the magnet output coil (coil #5) at a higher current and magnetic field, to explore field shaping to inhibit beam radial growth and reduce body current, was proposed by CPI. A definitive successful demonstration might influence the design of future solenoids. A more modest initial experiment was conducted, varying the magnet current to all coils by ~ ± 1 A about the NPV value I_M = 22 A. Changes to body current and thermal dissipation were small, with no compelling trends, confirming the NPV value for I_M. The more comprehensive experiment was not undertaken, an example of the more detailed test program that was anticipated for the prototype but not completed because SN 110 was placed in service as an operational unit in response to another VKX-7864B tube failure in July 2017.

NASA SMD concurred with a no-cost extension of the task plan and CPI deferred the final milestone payments of their subcontract to accommodate the delay in completion of JPL acceptance testing.

VI. Performance Testing

Performance testing examines how the klystron will perform as a key element of the GSSR and was defined to be a JPL responsibility, outside the scope of the CPI subcontract. Performance testing consists of:

(1) Phase linearity measurement.

(2) Group delay measurement.

(3) In-band spurious output testing.

(4) GSSR ranging modulation testing.

Harmonic output testing, originally planned, could not be accomplished because an appropriate GSSR-specific filter was unavailable. Although important for klystrons used in spacecraft telecommunication transmitters, this measurement was deemed less important for a transmitter system used for radar astronomy, and may reflect a requirements inconsistency that should be corrected in the technical specifications document prior to production of a set of operational klystrons.

Figure 17 shows the phase deviation in degrees as a function of frequency and an estimate of the phase linearity. The blue line is the measured data acquired with a network analyzer. The red lines are the closest pair of parallel lines, with the slope of the best fit straight line to the data, that bound the envelope of phase deviation over the 50-MHz frequency range of interest. A functional definition of linearity, $\Delta\alpha$, is the maximum phase deviation from the best linear fit, approximately half the phase difference between the parallel lines. By this definition, the linearity $\Delta\alpha = \pm$ 21.7 deg of phase. Over the central 18 MHz, $\Delta\alpha = \pm$ 4.7 deg of phase. These values are somewhat larger than requirements, ± 15 deg and ± 3 deg of phase deviation, respectively. A 15-deg phase offset between the response of two klystrons operating at a single frequency in CW mode would result in 98.3 percent transmitted power; that is, nearly perfect power combining for a two-klystron system like the GSSR.

The group delay measurements were not definitive. A variation in group delay of ~12 ns was estimated over the frequency range 8540–8580 MHz, which corresponds to the maximum 40-MHz chirp modulation bandwidth currently employed in the highest-resolution GSSR mode. This will lead to range smearing of ~1.8 m in a delay-Doppler image, about half a 3.75-m range bin.

The in-band spurious output test consisted of a search for spurs in the klystron's output noise power spectrum. Intermodulation products with 400 Hz (motor generator frequency) and 60 Hz (filament power supply frequency) were observed at –56 dBc and –52 dBc, respectively. All other spurs were down at least –100 dBc, meeting requirements.

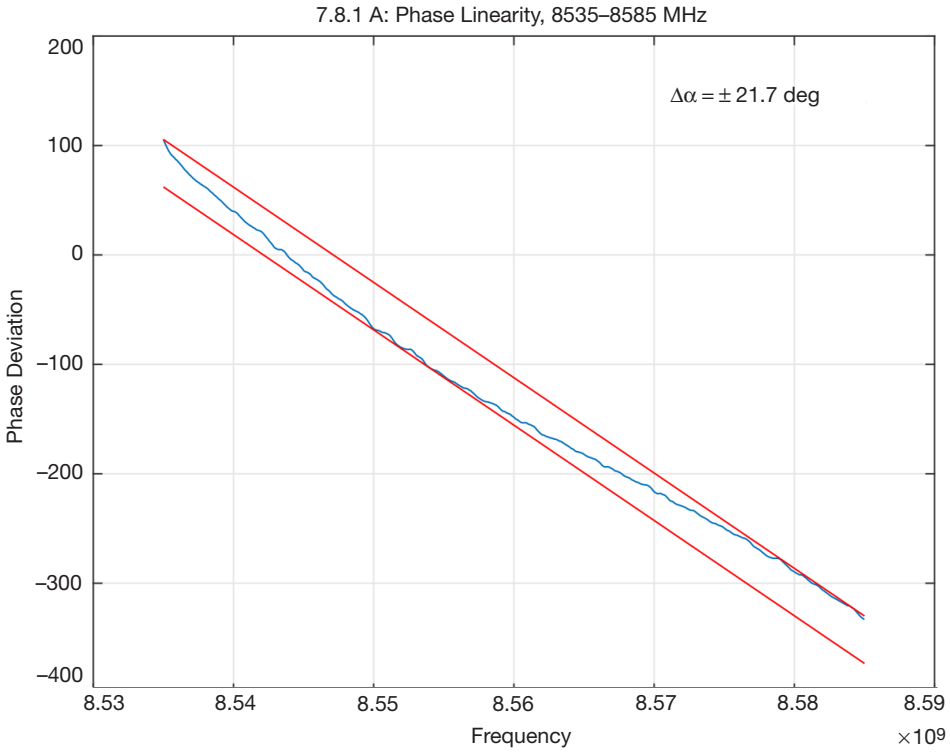

Figure 17. Phase deviation over 50-MHz bandwidth. The departure from linearity is small, resulting in excellent power combining in a two-klystron transmitter system.

Figures 18 and 19 show output power P_o as a function of frequency for two standard GSSR ranging modulations, binary phase code (BPC) at 1/8 microsecond (µs) and 1/20 µs baud rate, respectively. At 1/8 µs, P_o = 280 kW, body current I_{by} = 35 mA, and the klystron body power dissipation was 7.7 kW. At 1/20 µs, P_o = 270 kW, I_{by} = 35.2 mA, and the klystron body power dissipation was 7.2 kW.

Figures 20 and 21 show output power P_o as a function of frequency for linear frequency modulation (LFM or "chirp") ranging modulations with a 20-µs sweep period and 50- and 60-MHz bandwidth, respectively. The chirp spectra are virtually flat and exhibit the sharp rolloff and low out-of-band sidelobe levels that make chirp a desirable modulation for high-resolution ranging and delay-Doppler imaging. For the 50-MHz spectrum, P_o = 271 kW, I_{by} = 26 mA, and the klystron thermal power dissipation was 7.3 kW. For the 60-MHz spectrum, P_o = 267 kW, I_{by} = 28 mA, and the klystron thermal power dissipation was 7.3 kW.

These measurements were among the first attempts to quantify if GSSR ranging modulations are more stressful than CW transmissions; that is, result in higher body current and a higher heat load needing effective dissipation without compromising klystron operational lifetime.

For all GSSR modulations, the VKX-7864C klystron readily produced P_o greater than ~270 kW, with I_{by} less than ~35 mA, easily meeting the not-to-exceed 70-mA body current requirement with modulation. A temperature increase of ~1.6 deg C across the body cooling circuit was reported for all cases. Approximately 0.4 to 0.5 µA of vacuum current was

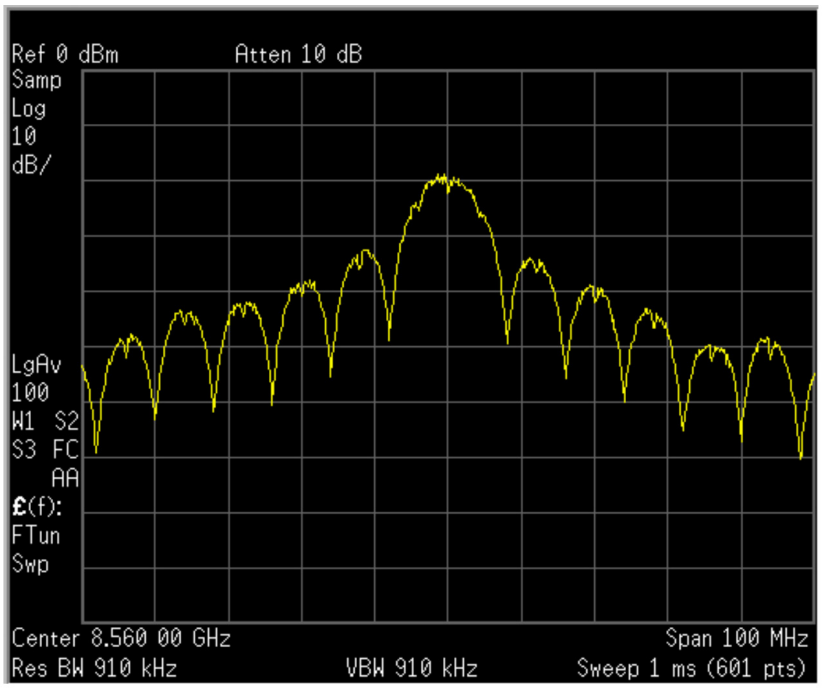

Figure 18. Output power P_o as a function of frequency for a BPC modulation with a 1/8-µs baud rate.

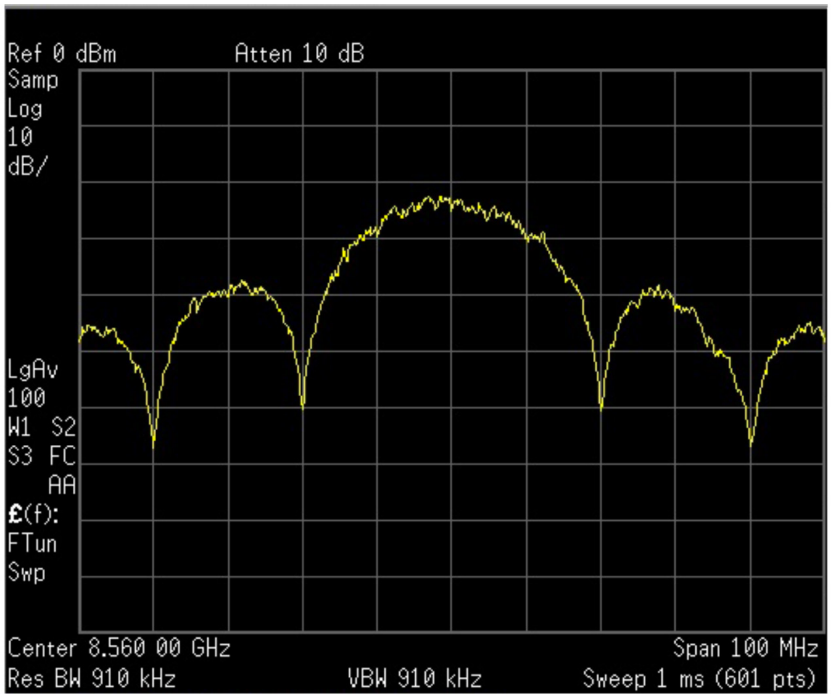

Figure 19. Output power P_o as a function of frequency for a BPC modulation with a 1/20-µs baud rate.

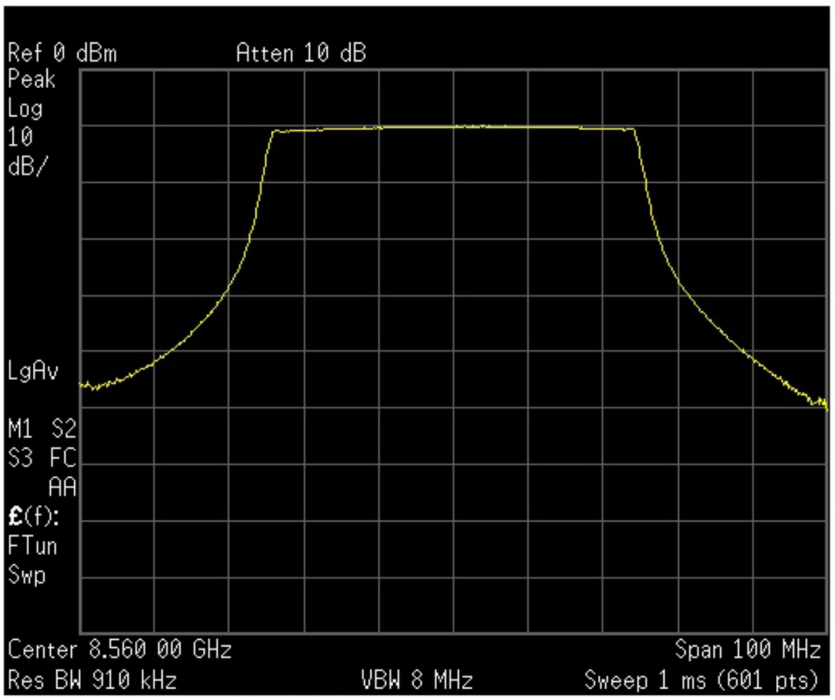

Figure 20. Output power P_o as a function of frequency for a chirp modulation with a 50-MHz bandwidth.

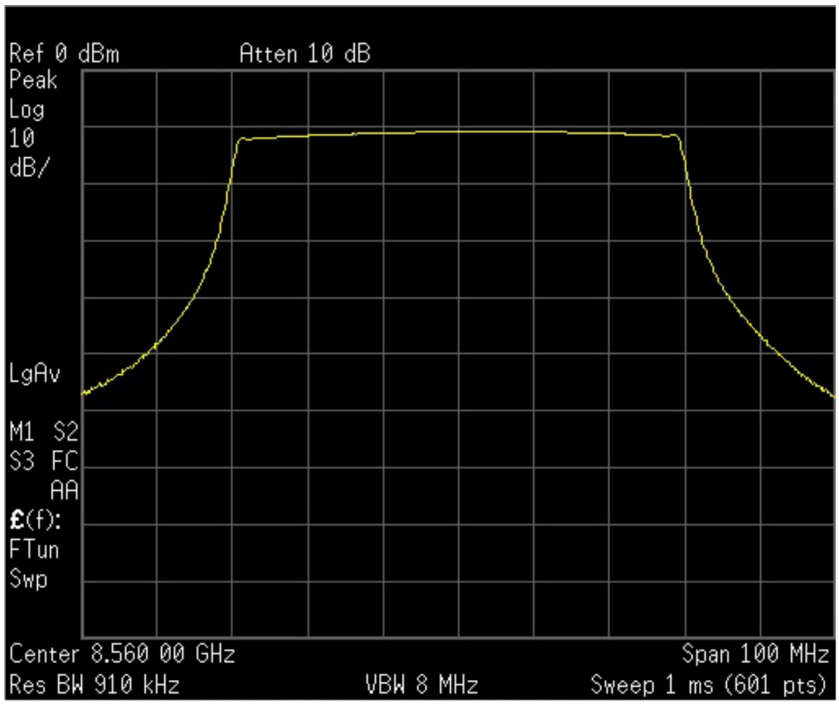

Figure 21. Output power P_o as a function of frequency for a chirp modulation with a 60-MHz bandwidth.

observed during modulations, slowly pumping down, indicating that tube conditioning was not complete, normal for a new device with limited operational hours. An important lesson learned: processing and conditioning the VKX-7864C SN 110 with GSSR modulations was important for elimination of residual trace gases — CW conditioning was insufficient and a slightly "gassy" tube was delivered. Processing and conditioning future operational devices with GSSR ranging modulations would be a better CPI practice for building a set of next-generation klystrons based on the new design.

Performance testing was completed on June 23, 2017, and the final test report was submitted to SMD on June 27, marking the formal conclusion of the KEMD task.

VII. Next Steps

Although the VKX-7864C SN 110 klystron, the first article prototype, was not intended as a spare for the operational GSSR transmitter, failure of one of the operational tubes reduced the GSSR to half-power operation. Facing a full schedule of scientific observations, the fastest way to restore the GSSR to full power was to press SN 110 into service, pairing it with one of the remaining VKX-7864B devices, taking advantage of an installation, integration, and testing opportunity afforded by a planned DSS-14 maintenance downtime. The first article prototype was installed on July 26, 2017. The weight of the complete device, the klystron itself plus the focusing solenoid magnet, was just under 1000 lb, the capacity limit of the DSS-14 service hoist. The tube and magnet were lifted to the main reflector separately and reintegrated on the dish prior to installation. Figure 22 shows the klystron installed on the DSS-14 antenna in the R&D cone that houses DSN radar and radio astronomy instrumentation.

Figure 23 shows a successful test result verifying the transmitter configuration with SN 110 of the new design in klystron socket #1, paired with an older klystron from the VKX-7864B model. Note the lower drive power P_d = 1.36 W of the new tube, operating at much lower power than it produces at its NPV drive power.

After DSS-14 was returned to operational service following the maintenance downtime, the GSSR conducted its first science observations. On August 9, 2017, the first echoes were returned with the new transmitter configuration. GSSR, back in service at full power, detected NEA 2001 QP153 in CW mode, with a calibrated transmitter power of 465 kW.

Based on the successful development of the VKX-7864C under the KEMD task, procurements have been initiated for the first two operational devices. The new klystron will be a key element of the future of the GSSR.

Figure 22. VKX-7864C SN 110 installed in the R&D cone on DSS-14, in klystron socket #1.

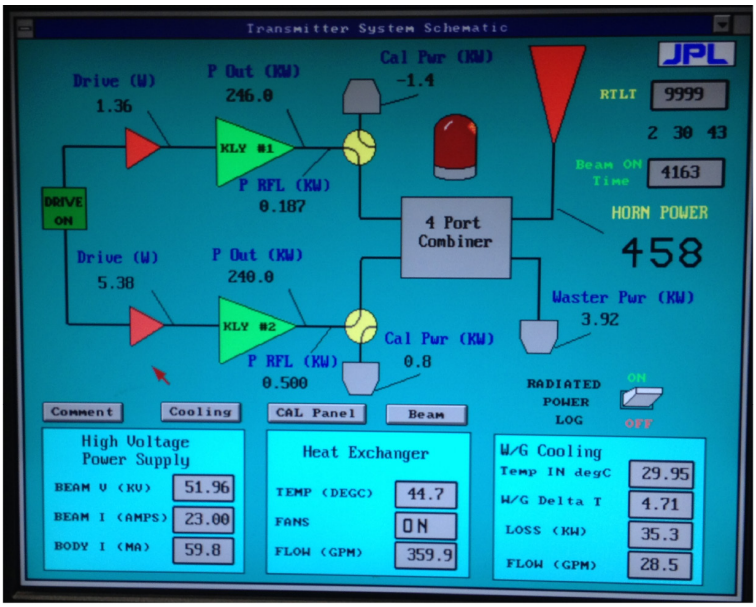

Figure 23. GSSR transmitter control interface showing a combined output power to the radiating feedhorn of 458 kW for a 40-MHz chirp modulation. The VKX-7864C first-article prototype is installed as klystron #1, operating at less than full power at an RF drive power P_d = 1.36 W.

Acknowledgments

The research described in this article was carried out in partnership with Communications & Power Industries (CPI). The JPL authors acknowledge the key role of the CPI engineering design team, consisting of Edward L. Eisen, Rasheda Begum, Brad Stockwell, Steve Cauffman, Alex Waggoner, Gaylen Aymar, Scott Forrest, Lou Zitelli, and Armand Staprans.

References

[1] J. L. Margot, S. J. Peale, R. F. Jurgens, M. A. Slade, and I. V. Holin, "Large Longitude Libration of Mercury Reveals a Molten Core," *Science*, vol. 316, p. 710, May 4, 2007.

[2] J. L. Margot, S. J. Peale, S. C. Solomon, S. A. Hauck II, Frank D. Ghigo, et al., "Mercury's Moment of Inertia from Spin and Gravity Data," *Journal of Geophysical Research*, vol. 117, p. E-1, October 2012.

[3] M. Brozovic, L. A. M. Benner, C. Magri, D. J. Scheeres, Michael W. Busch, et al., "Goldstone Radar Evidence for Short-Axis Mode Non-Principal-Axis Rotation of Near-Earth Asteroid (214869) 2007 PA8," *Icarus*, vol. 286, p. 314, 2017.

[4] M. Brozovic, R. S. Park, J. G. McMichael, J. D. Giorgini, M. A. Slade, et al., "Radar Observations of Spacecraft in Lunar Orbit," International Symposium in Space Technology and Science, 2017.

[5] D. J. Mudgeway, *Uplink–Downlink: A History of the Deep Space Network 1957–1997*, SP-2001-4227, The NASA History Series, NASA Office of External Relations, 2001.

[6] R. Cormier and A. Mizuhara, "250-kW CW Klystron Amplifier for Planetary Radar," *The Telecommunications and Data Acquisition Progress Report*, vol. 42-108, Jet Propulsion Laboratory, Pasadena, California, pp. 1–13, February 15,1992. http://ipnpr.jpl.nasa.gov/progress_report/42-108/108O.PDF

[7] A. Mizuhara, "Bandwidth and Group Delay Extension for an X-band 250 kW CW Klystron for JPL/NASA Deep Space Radar," *Proceedings of the IEEE 5th Conference on Vacuum Electronics,* pp. 77–78, April 2004.

[8] National Research Council, *Defending Planet Earth: Near-Earth Object Surveys and Hazard Mitigation Strategies*, Washington, DC: The National Academies Press, 2010.

[9] J. R. Brophy, L. Friedman, and F. Culick, "Asteroid Retrieval Feasibility Study," sponsored by Keck Institute for Space Studies, *Proceedings of the IEEE Aerospace Conference*, pp. 1–16, 2012.

[10] A. Balkcum, A. Mizuhara, B. Stockwell, R. Begum, L. Cox, et al., "Design and Operation of a 100 kW CW X-band Klystron for Spacecraft Communications," *IVEC 2012 Conference Proceedings*. IEEE, pp. 315–316, April 2012.

[11] T. Habermann, A. Balkcum, R. Begum, H. Bohlen, M. Cattelino, et al., "High-Power Test Results of a 10 MW, High Efficiency, L-band Multiple Beam Klystron," *Proceedings of PAC09,* no. WE3RAC03, Vancouver, BC, Canada, 2009.

[12] T. Habermann, A. Balkcum, R. Begum, H. Bohlen, M. Cattelino, et al., "High-Power, High-Efficiency L-band Multiple-Beam Klystron Development at CPI," *IEEE Transactions on Plasma Science*, vol. 38, no. 6, p. 1264, June 2010.